Effect of Deep Level Impact Ionization on Avalanche Breakdown in Semiconductor p−n Junctions

Samsoo Kang and Charles W. Myles

Department of Physics and Engineering Physics, Texas Tech University, Lubbock, Texas 79409-1051, USA

(Received October 6, 1999; in revised form June 14, 2000)

Using a simple model, we have investigated the effect of deep level impact ionization on avalanche breakdown in GaAs, InP, and Si p−n junctions. The ionization coefficients are obtained using Robbins' formalism [phys. stat. sol. (b) **97**, 9 (1980)]. Results are presented for trends in the dependence of the breakdown voltage and electric field on the doping densities and on the deep level density and energy. Our results show that, for fixed doping densities, the breakdown voltage and field both decrease with increasing deep level density. Further, we find that their sensitivity to the deep level density is much stronger for levels deep within the bandgap than for those near a band edge, correlating with the decreased ionization threshold energy for shallower levels. We also find that the breakdown voltage and critical field in Si p−n junctions are stronger functions of the deep level density and energy than in GaAs and InP junctions.

1. Introduction

The avalanche breakdown voltage is an important characteristic of high voltage semiconductor devices. Microscopically, this breakdown is initiated by impact ionization [1]. Various ionization mechanisms can contribute, yet few studies have been made to determine their relative importance, and most theories have only considered the band-to-band mechanism. In this paper, we present a model calculation of the trends in the effects of deep level impact ionization on avalanche breakdown in GaAs, InP, and Si p−n junctions.

The properties of a semiconductor can be strongly influenced by deep levels in the bandgap [2], and deep levels can have a major effect on the avalanche breakdown properties of the material [3 to 8]. For example, for photoconductive switches, the observed breakdown voltage is lower than expected on the basis of band-to-band ionization alone [3 to 6]. A possible cause of this is deep level impact ionization.

Avalanche breakdown in p−n junctions has been well-studied theoretically [9, 10] and experimentally [11], and experiments have been performed in which deep level effects on junction breakdown have been considered [12]. To our knowledge, except for the work in Ref. [13], which considered the impact ionization of traps in GaAs field effect transistors, the effect of deep level impact ionization has not been included in theoretical studies of p−n junction breakdown. In this paper, we include this effect using simple models of the junction and of the ionization coefficients. Our model is similar to Hauser's [9] junction breakdown model, but the impact ionization coefficients are obtained from Robbins' [14] formalism and the deep level density is added to the doping densities in the electric field computation. This formalism treats band-to-band

and deep level ionization on the same footing and allows a detailed study of avalanche breakdown with both mechanisms included. The ionization coefficients are obtained numerically using experimental and theoretical material parameters in the formalism. With this model, one can obtain trends in the dependence of the breakdown properties on the doping densities and on the deep level density and energy.

Our model is strictly valid for hydrogenic impurities. Thus, its application to deep levels should be regarded as an approximation. Further, it is simple enough that its predictions for breakdown voltages and related properties should be viewed as only first estimates. More sophisticated theoretical tools, such as drift diffusion models [1] and Monte Carlo simulations [15], could be applied to this problem. These may give more reliable quantitative information than the present approach. However, implementing these would require considerable computational effort. Rather than absolute numbers, the goal of this study is to obtain trends for the dependence of the breakdown properties on the deep level density and energy.

2. Background and Theory

The theory of impact ionization has a long history. A central issue is to determine the ionization coefficient, $\alpha(E)$, which is proportional to the probability that a charge carrier in an electric field E gains an energy exceeding a given threshold. Early attempts to calculate $\alpha(E)$ microscopically were the high-field model of Wolff [16] and the low-field model of Shockley [17].

An early impact ionization theory was developed by Baraff [18], who used the Boltzmann equation to numerically obtain $\alpha(E)$. This theory assumes breakdown due to band-to-band ionization only and energy loss through optical phonon emission. There have been several extensions of Baraff's theory [19], and this model and its extensions were widely used in early breakdown studies. Crowell et al. [20] developed an analytical expression for $\alpha(E)$ to approximate Baraff's numerical results. It has been used by Hauser [9] and by Hur et al. [10] in their studies of junction breakdown due to band-to-band ionization. Robbins [14], as part of his general treatment of impact ionization and breakdown, developed closed form expressions for $\alpha(E)$ for both band-to-band and deep level ionization. We use this formalism here.

2.1 Breakdown conditions and impact ionization coefficients

If both band-to-band and deep level ionization are included, avalanche breakdown is determined by the voltage for which the following expression holds [1, 14]

$$\int_{-x_\mathrm{n}}^{x_\mathrm{p}} (\alpha_\mathrm{n} + \alpha_\mathrm{tn}) \exp\left[-\int_{x}^{x_\mathrm{p}} (\alpha_\mathrm{n} - \alpha_\mathrm{p})\, \mathrm{d}x' \right] \mathrm{d}x = 1\,, \tag{1}$$

where α_n, α_p are the electron and hole band-to-band impact ionization coefficients, α_tn is the coefficient for electron impact ionization from a deep level, $-x_\mathrm{n}$, x_p are the depletion region boundaries, and the abrupt junction is at $x = 0$. (An equivalent expression, obtained from Eq. (1) by interchanging α_n and α_p, by changing the lower limit of integration in the argument of the exponential to $-x_\mathrm{n}$ and the upper limit to x, and by replacing α_tn with α_tp, the ionization coefficient for hole ionization from a trap, could also be used.) Here and in what follows, quantities with subscripts n and p denote properties of the n-type and of the p-type material, respectively.

In order to evaluate Eq. (1), the dependences of the ionization coefficients on the electric field $E(x)$ are needed. For both band-to-band and deep level ionization, we use the expressions for $\alpha(E)$ obtained from Robbins' [14] formalism. We note that this approximation is especially weak for GaAs [14]. The Robbins expressions for $\alpha(E)$ depend on the electron and hole effective masses m_e and m_h, the optical phonon mean free path λ, the bandgap ε_g, the dielectric constant ϵ, the electron and hole ionization threshold energies ε_T^e and ε_T^h, and the electric field-dependent electron and hole drift velocities, $v^e = v^e(E)$ and $v^h = v^h(E)$. The coefficients for deep level ionization also depend on the deep level density N_T and the deep level energy ε_t.

To compute the drift velocities and threshold energies, we use the models described below. The other parameters are obtained from published experimental [1] and theoretical [20 to 31] data. These data are summarized in Table 1. The deep level energy and density are treated as variable parameters. In all calculations, we have used the room temperature value of the (temperature dependent) phonon mean free path.

Table 1

Parameters ($T = 300$ K) used in breakdown calculations

parameter	symbol	GaAs	InP	Si
dielectric constant [1]	ϵ	13.2	11.1	11.9
minimum band gap (eV) [1]	ε_g	1.42	1.34	1.12
phonon mean free path (Å)	λ	50.0 [9]	45.2 [9]	44.0 [31]
relative effective mass [1]				
electron	m_e	0.067	0.079	0.68 [1])
hole	m_h	0.68	0.46	0.55 [2])
threshold energy (eV)				
electron	ε_T^e	1.55	1.49	1.09
hole	ε_T^h	2.74	2.35	1.99
saturation drift velocity (10^7 cm/s) [1]				
electron	v_s^e	0.63	0.75	1.00
hole	v_s^h	1.02	0.70	0.80
maximum drift velocity (10^7 cm/s) [1]				
electron	v_p^e	2.02	0.26	1.00
hole	v_p^h	1.02	0.80	0.80
peak drift velocity field (10^4 V/cm) [1]				
electron	E_p^e	0.38	12.4	6.50
hole	E_p^h	7.00	10.0	50.0
low field mobility (10^2 cm^2/Vs) [1]				
electron	μ_L^e	80.0	60.0	14.0
hole	μ_L^h	4.51	1.50	4.60
drift velocity parameter [22]	σ	0.20	0.17	0.05

[1]) $m_e = 3^{2/3}(m_l m_t^2)^{1/3}$
[2]) $m_h = (m_{hh}^{3/2} + m_{lh}^{3/2})^{2/3}$

2.2 Drift velocity

At low fields, the drift velocity is a linear function of field. As the field increases, the velocity becomes a strong function of field, and, at high enough fields, saturates to an approximately constant value. For some materials, such as GaAs, as the field increases, the velocity reaches a peak value and then decreases before saturation. These effects are due to the fact that higher energy, satellite valleys in the conduction bands become populated at high fields [1].

If a purely microscopic description is desired, a closed form expression for this field dependence of the drift velocity is not possible. However, here, in keeping with our simple model approach, we will use a phenomenological expression for this field dependence. A commonly used closed form model for the drift velocity was developed by Caughey and Thomas [22]. In the simplest form of this model, the velocity is written as $v_C(E) = \mu_L E / [1 + (\mu_L E / v_s)]$, where μ_L is low field mobility, and v_s is the drift velocity at saturation. The hole drift velocity is not well described by this model [22].

Here, we have used a unified model, suggested by Mohammad [23], for the field dependence of the electron and hole drift velocities. It is a generalization of the Caughey-Thomas model in which the drift velocity takes the form

$$v(E; \sigma) = v_C(E) + [v_p - v_C(E_p)] \exp\left[-5.1\left|(E_p/E)^\sigma - 1\right|\right], \qquad (2)$$

where v_p is the velocity at the peak in the v versus E curve, E_p is the value of E at this peak, and σ is an adjustable parameter. In a material, such as Si, where the v versus E curve saturates without peaking, $v_p = v_s$. The values of μ_L, v_s, v_p, E_p, and σ for electrons and holes in GaAs, InP, and Si, which we have used for electrons are shown in Table 1.

2.3 Ionization threshold energy

There have been many models of the impact ionization threshold energy ε_T [24 to 27]. These have utilized various approximations for the bands, from simple parabolic bands [24] to realistic pseudopotential bands [25, 26]. In our calculations, we have used Hauser's model [24]. It assumes single parabolic valence and conduction bands and computes ε_T by requiring momentum and energy conservation in the ionization process. This gives closed form solutions for ε_T in both direct and indirect band gap materials [24]. The quantities needed in this model are the electron and hole effective masses and (for indirect gap materials) the lattice constant. The ionization threshold energies for electrons and holes in GaAs, InP, and Si, obtained using the band gaps and effective masses from Table 1 in this formalism are also listed in Table 1.

For ionization of an electron from a deep level, the threshold energy is the difference between the bandgap and the deep level energy. For ionization of a hole from a deep level, the threshold energy is the deep level energy. In both cases, it is assumed that the zero of energy is the top of the valence band.

2.4 Critical field and breakdown voltage

Our model for the p–n junction is a modification of the usual abrupt junction model [1] to include deep level effects. In this model, under steady state conditions, the electric

field $E(x)$ at position x in the junction is given by

$$\frac{\epsilon}{e}\, E(x) = \begin{cases} (N_D + N_T)\, x_n \left(1 + \dfrac{x}{x_n}\right), & -x_n \leq x \leq 0 \\[2mm] (N_A + N_T)\, x_p \left(1 - \dfrac{x}{x_p}\right), & 0 \leq x \leq x_p \end{cases}, \tag{3}$$

where N_D and N_A are the donor and acceptor densities and N_T is the deep level density. Boundary conditions at $x = 0$ require that $(N_D + N_T)x_n = (N_A + N_T)\, x_p \equiv \frac{\epsilon}{e}\, E_m$. Here E_m is the critical field. The breakdown voltage is obtained from $V_B = \frac{1}{2}\, E_m(x_n + x_p)$.

For a level density N_T which is small compared with the doping densities N_D and N_A, the effect of the deep levels on the depletion region boundaries x_n and x_p is small, and, to a good approximation, Eq. (3) reduces to the abrupt junction model. In this case, one can calculate the effects of deep level ionization on the breakdown properties and the dependences of these properties on the deep level density N_T and energy ε_t using the depletion region boundaries determined by the doping densities alone.

On the other hand, for a level density which is comparable to one of the doping densities, the energy bands near the junction are modified. For example, Schibli et al. [28] and Sah et al. [29] have calculated the bands near p^+–n and n^+–p junctions for some specific materials and deep levels. They find band bending near the junction, resulting in a graded junction. They also find that the bands change with the doping and deep level densities. These complications make it difficult to calculate the breakdown properties of a junction with a high deep level density in a general way.

In most of what follows, we have calculated the junction breakdown properties for cases where the deep level density is small compared with the doping densities. Thus, we have used the abrupt junction formalism without further approximation. To look at a representative case where the deep level density is comparable to one of the doping densities, we have assumed that the junction is an In doped n^+–p junction in Si. Since this is known to be an abrupt junction to a good approximation [30], we have also used the abrupt junction approximation in this calculation. In this case, we also compare our results to those of Sah [30] for the same junction.

3. Results

We have used the model just described to study the effects of band-to-band and deep level impact ionization on avalanche breakdown in GaAs, InP and Si p–n junctions. We have computed the critical field and breakdown voltage for a variety of doping and deep level densities and for several deep level energies. In order to help to clarify the relative importance of band-to-band and deep level ionization, we have done some calculations including both effects and some including only band-to-band ionization.

3.1 Band-to-band ionization

Typical results, including only band-to-band ionization, are shown in Fig. 1. Figures 1a and b show our predictions for the maximum electric field E_m and the breakdown voltage V_B as functions of doping density. The results for GaAs, InP, and Si junctions are shown as solid, short-dashed, and long-dashed curves, respectively. These are similar to results obtained by others [9, 10, 31].
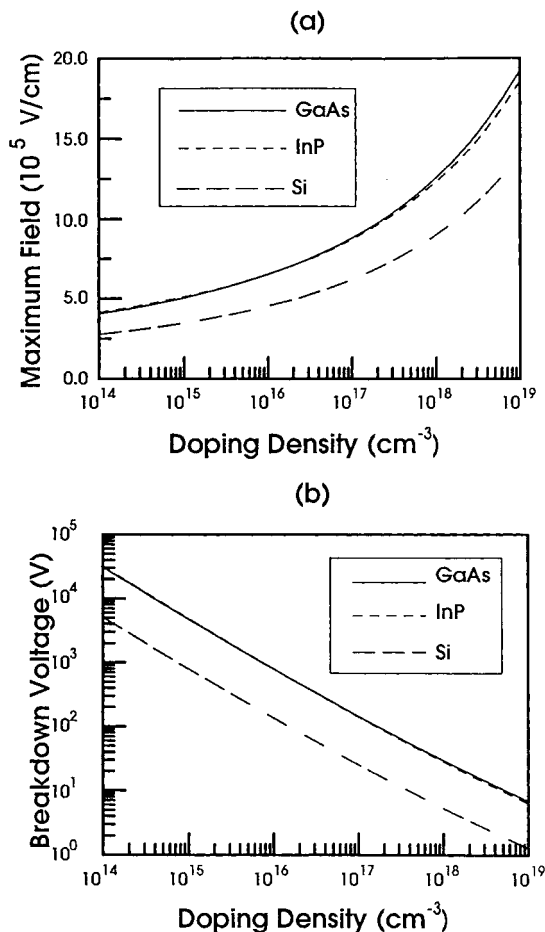
(a)

Fig. 1. Predicted doping density dependence of avalanche breakdown properties of GaAs (solid curves), InP (short-dashed curves), and Si (long-dashed curves) p–n junctions, including band-to-band impact ionization only. a) Critical field; b) breakdown voltage

(b)

As can be seen in Fig. 1a, the predicted breakdown field is an increasing function of doping density. In Fig. 1b, it can be seen that the breakdown voltage is a decreasing function of doping density. This can be understood by noting that the depletion layer width $x_p + x_n$ is a strongly decreasing function of doping density [9, 10]. Thus, impact ionization becomes more likely as the doping density is increased. From Figs. 1a and b, it can be seen that the breakdown properties for GaAs junctions are very similar to those for InP junctions. This is because these materials have similar electronic properties. The breakdown properties for Si junctions are qualitatively similar to but quantitatively different from those of the other materials. These differences are primarily due to the differences in the electronic properties of Si and the other materials. Within the present model, these differences are primarily due to the different mobilities and drift velocities in the materials considered. However, they also are influenced by the different bandstructures of the materials as well (direct vs. indirect bandgap, etc.).

3.2 Band-to-band plus deep level ionization; low deep level density

To explore deep level impact ionization effects on junction breakdown, we have computed the breakdown voltage and critical field as functions of deep level density for GaAs, InP, and Si junctions, for several doping densities and deep level energies. As for band-to-band ionization, the results for GaAs and InP are qualitatively and quantitatively very similar – thus, here we show our results for a GaAs junction only. Typical results in the case where the deep level density is small compared to the doping densities are shown in Figs. 2 and 3, which are results for GaAs and Si p–n junctions. In those figures, the doping densities have been fixed at $N_D = N_A = 10^{17}$ cm^{-3} and the
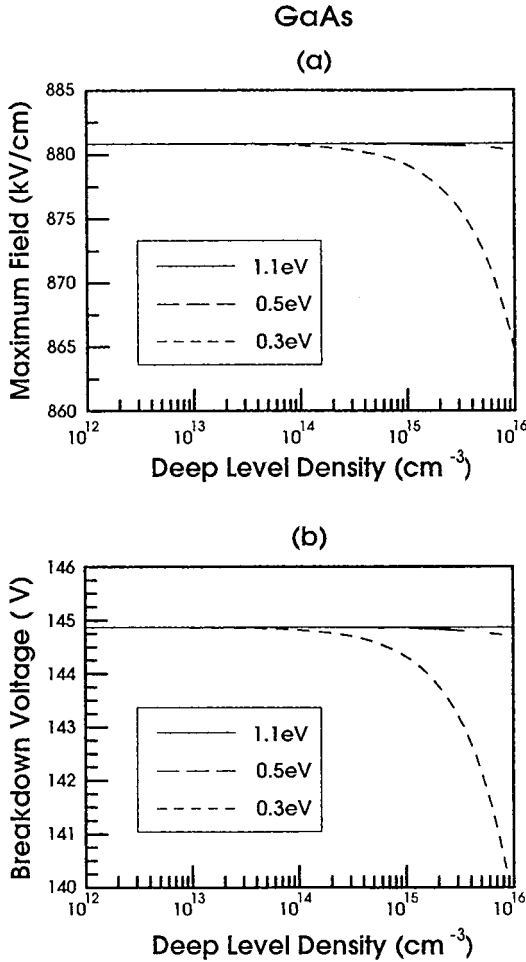
GaAs

(a)

Fig. 2. Predicted avalanche breakdown properties of a GaAs p–n junction, including band-to-band and deep level impact ionization. The doping densities are fixed at $N_A = N_D = 10^{17}$ cm^{-3} and the deep level density N_T has been assumed to be small in comparison with this. The critical field and breakdown voltage are shown as functions of deep level density for deep level energies of 1.1 eV (solid curves), 0.5 eV (long-dashed curves), and 0.3 eV (short-dashed curves). a) Critical field; b) breakdown voltage

(b)

deep level density is varied from 10^{12} to 10^{16} cm^{-3}. Results for the critical field are shown in Figs. 2a and 3a, while Figs. 2b and 3b show results for the breakdown voltage. Results are shown for three deep level energies: $\varepsilon_t = 1.1$ eV (solid curves), 0.5 eV (long-dashed curves), and 0.3 eV (short-dashed curves). Here, and in all subsequent results, ε_t is measured with respect to the top of the valence band, which we have taken to be the zero of energy.

Figure 2a shows the critical field in a GaAs p–n junction as function of deep level density for the three level depths mentioned. As can be seen, as the deep level moves down from the conduction band and as the level density increases, no significant change in the critical field is predicted until the level reaches ~ 0.5 eV, at a density of $\sim 10^{15}$ cm^{-3}. For larger densities, the critical field is predicted to be a decreasing function of level density. For deeper levels, this effect becomes important for smaller level densities. The dependence on level depth can be understood from Robbins' impact ionization formalism [14], in which the deep level impact ionization coefficient contains a pre-exponential factor which is inversely proportional to the square of the deep level ionization threshold energy. This coefficient is, however, dominated by its exponential dependence on this energy. The combined effect is such that, taking electron and hole ionization together, as the depth below the conduction band increases, impact ionization becomes more probable, decreasing the critical field. The dependence of the critical field on the level density can be understood by noting that the ionization coefficient is proportional to that density. From Fig. 2a, for $\varepsilon_t = 0.3$ eV, and for a level density of 10^{12} cm^{-3}, the

predicted critical field for breakdown in a GaAs junction is ≈ 881 kV/cm. As the level density increases, the critical field decreases, and, for this same deep level, it becomes ≈ 865 kV/cm at a level density of 10^{16} cm^{-3}.

Figure 2b shows the predicted breakdown voltage in a GaAs p–n junction as a function of deep level density for the three mentioned level depths. As can be seen, the breakdown voltage has the same trends with level density and depth as the critical field. This can be understood by noting that the depletion width $x_n + x_p$ is independent of these quantities. As can be seen in this figure, as the deep level moves down from the conduction band and as the level density increases, no significant change in the breakdown voltage is predicted until the depth reaches ~ 0.5 eV, at a level density of $\sim 10^{15}$ cm^{-3}. For larger level densities, the breakdown voltage is a decreasing function of level density. For deeper levels, this effect becomes important at smaller level densities. For $\varepsilon_t = 0.3$ eV and $N_T = 10^{12}$ cm^{-3}, the breakdown voltage is predicted to be ≈ 145 V. For this same deep level, it becomes ≈ 140 V at a level density of 10^{16} cm^{-3}.

Figures 3a and b show the predicted critical field and breakdown voltage for a Si p–n junction as a function of deep level density for deep levels at $\varepsilon_t = 1.1, 0.5$, and 0.3 eV. These have similar trends as for GaAs junctions. However, there are quantitative differences, due to the differences in the electronic properties of Si and GaAs. In particular, Si has an indirect bandgap and a lower threshold energy for band-to-band ionization. Thus, the band-to-band ionization coefficients $\alpha(E)$ for Si are larger than for GaAs. Therefore, breakdown can take place more easily in Si and the critical field and breakdown voltage are lower than in GaAs. Further, for Si junctions, the critical
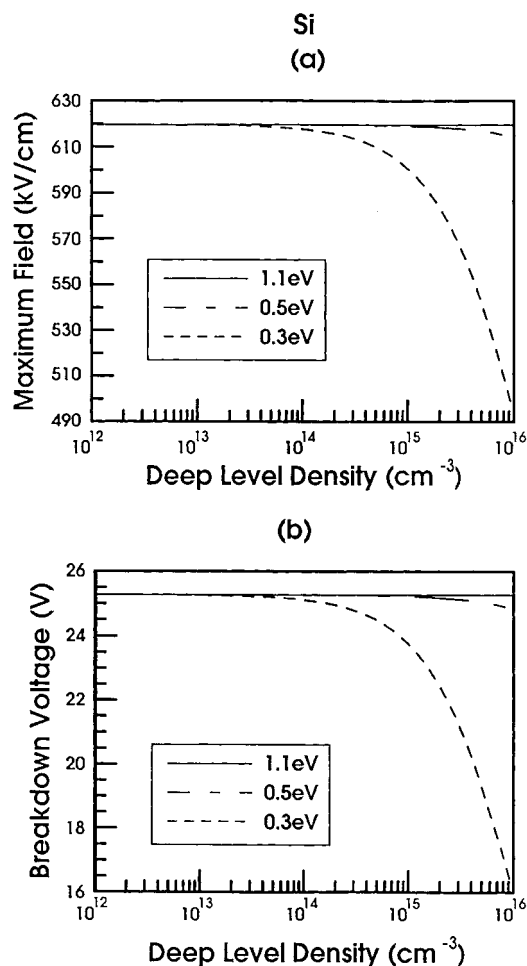

Fig. 3. Predicted avalanche breakdown properties of a Si p–n junction, including band-to-band and deep level impact ionization. The doping densities are fixed at $N_A = N_D = 10^{17}$ cm^{-3} and the deep level density N_T has been assumed to be small in comparison with this. The critical field and breakdown voltage are shown as functions of deep level density for deep level energies of 1.1 eV (solid curves), 0.5 eV (long-dashed curves), and 0.3 eV (short-dashed curves). a) Critical field; b) breakdown voltage

field and breakdown voltage are more sensitive functions of the deep level density and energy than in GaAs.

As can be seen from Figs. 3a and b, for small deep level densities, E_m and V_B remain unchanged in the presence of deep levels (as is intuitive). However, as the deep level moves down from the conduction band and as the deep level density begins to increase, both the critical field and the breakdown voltage in a Si p–n junction begin to decrease. This effect becomes noticeable at a level energy of 0.5 eV and at a level density of $\sim 10^{15}$ cm^{-3}. When the level energy has reached 0.3 eV, the decrease in critical field and breakdown voltage are noticeable at level densities as low as $\sim 10^{14}$ cm^{-3}. For $\varepsilon_t = 0.3$ eV and for a level density of 10^{12} cm^{-3}, E_m and V_B are predicted to be ≈ 620 kV/cm and ≈ 25 V. For the same deep level, at a level density of 10^{16} cm^{-3}, they are predicted to be ≈ 490 kV/cm and ≈ 16 V.

3.3 Si n$^+$–p junction; deep level density comparable to doping density

Figures 4a and b show the predicted critical field and breakdown voltage for a Si n$^+$–p junction as a function of deep level density. In this case the deep level density has been varied until it is comparable to one of the doping densities. In Fig. 4, the doping densities have been fixed at $N_D = 10^{17}$ cm^{-3} and $N_A = 2 \times 10^{16}$ cm^{-3}. These results show similar trends as for the Si junction with higher acceptor density (Fig. 3), as long as the deep level density remains small in comparison with the doping densities. They deviate from those when the level density becomes comparable to one of the doping densities. From Figs. 4a and b, for a deep level at $\varepsilon_t = 1.1$ eV, the critical field and breakdown voltage
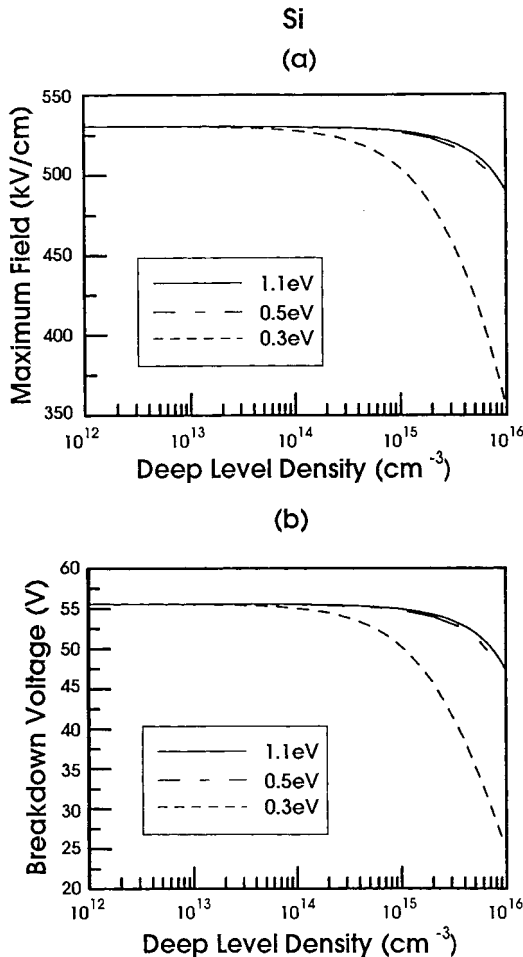

Fig. 4. Predicted avalanche breakdown properties of a Si n$^+$–p junction, including band-to-band and deep level impact ionization. The doping densities are fixed at $N_D = 10^{17}$ cm^{-3} and $N_A = 2 \times 10^{16}$ cm^{-3} and there is no restriction on the deep level density N_T. The predicted critical field and breakdown voltage are shown as functions of deep level density for deep level energies of 1.1 eV (solid curves), 0.5 eV (long-dashed curves), and 0.3 eV (short-dashed curves). a) Critical field; b) breakdown voltage

decrease as functions of level density and this effect is noticeable at a level density as low as $N_T = 10^{14}$ cm^{-3}. This should be contrasted with the almost constant behavior of these quantities with respect to the level density for the same deep level, shown in Fig. 3.

The behavior when the deep level density is comparable to one of the doping densities is caused by band edge bending at the junction and by the fact that the band edges are functions of the level density. Sah et al. [30] have calculated and measured the breakdown voltage as a function of deep level density for a Si n$^+$–p junction. They find that reciprocal of the breakdown voltage for a n$^+$–p junction increases linearly as the level density increases. This is in qualitative agreement with the trend predicted in Fig. 4.

4. Conclusions

We have investigated the effects of deep level impact ionization on avalanche breakdown in GaAs, InP, and Si p–n junctions. The ionization coefficients were obtained by combining Robbins' formalism [14] with simple models for the threshold energy and the drift velocity. Numerical results were obtained by inputting experimental and theoretical parameters into this model. Despite the simplicity of our model, we believe that the trends it predicts should be reliable.

Our results show that, for fixed doping densities, the critical field and breakdown voltage are decreasing functions of deep level density and energy. Further, we find that their sensitivity to increases in level density is much stronger for levels near mid-gap than for levels near a band edge. We also find that the breakdown voltage and critical field in Si junctions are more sensitive to changes in the deep level density and energy than they are in GaAs junctions. These results are in qualitative agreement with observations and other calculations [3 to 8, 30].

References

[1] S. Wang, Fundamentals of Semiconductor Theory and Device Physics, Prentice Hall, Englewood Cliffs (NJ) 1989 (pp. 416 to 420).
    S.M. Sze, Physics of Semiconductor Devices, Wiley, New York 1981.
[2] S.T. Pantelides, Deep Centers in Semiconductors, Gordon and Breach, New York/London 1986.
[3] D. Stoudt, K. Schoenbach, R. Brinkman, V. Lakdawala, and G. Gerdin, IEEE Trans. Electron Devices **37**, 2478 (1990).
    V. Lakdawala, S. Panigrahi, L. Thomas, and R. Brinkmann, Proc. SPIE **1632**, 120 (1992).
[4] G.M. Loubriel, F.J. Zutavern, W.D. Helgeson, D.L. McLaughlin, and M.W. O'Malley, in: Digest of Technical Papers, 8th Pulsed Power Conf., San Diego (CA), 1991, Eds. R. White and K. Prestwich, IEEE, New York 1991 (p. 33).
[5] J. Yee, G. Khanaka, R. Druce, and M. Pocha, Proc. SPIE **1632**, 21 (1992).
    C. Capps, Proc. SPIE **1632**, 254 (1992).
    L. Partain, D. Day, and R. Powell, J. Appl. Phys. **74**, 335 (1993).
[6] Z. Li, S. Aliste, W. McMullan, and C. Hurd, J. Appl. Phys. **67**, 7368 (1990).
    C. Li, T. Barton, and R. Miles, IEEE Trans. Electron Devices **40**, 811 (1993).

[7] Q.A. HUANG, J. Appl. Phys. **79**, 3703 (1996).
     H. KOSTIAL, K. PLOOG, R. HEY, and F.G. BOEBEL, J. Appl. Phys. **78**, 4560 (1995).
[8] A.V. DMITRIEV and A.B. EVLYUKHIN, Semicond. Sci. Technol. **9**, 2056 (1994).
     A. DARGYS and J. KUNDROTAS, Litov. Fiz. Sb. **34**, 395 (1994) [Lith. Phys. J. **34**, 345 (1994)].
     S.B. LASTOVSKII and I.G. MARCHENKO, Pisma Zh. Tekh. Fiz. **20**, 12 (1994) [Tech. Phys. Lett. **20**, 138 (1994)].
     I.N. YASSIEVICH and L.C. KIMERLING, Semicond. Sci. Technol. **8**, 718 (1993).
[9] J.R. HAUSER, Appl. Phys. Lett. **33**, 351 (1978).
[10] J.H. HUR, C.W. MYLES, and M.A. GUNDERSEN, J. Appl. Phys. **67**, 6917 (1990).
[11] V. DOBROVOLSKII and S.B. GRYAZNOV, Fiz. Tekh. Poluprov. **29**, 1453 (1995); **28**, 266 (1994); **26**, 1366 (1992) [Semicond. **29**, 757 (1995); **28**, 160 (1994); **26**, 766 (1992)].
[12] N. INOUE, A. ITOH, T. KIMOTO, and H. MATSUNAMI, J. Electron. Mater. **26**, 165 (1997).
     A.M. MINARSKII, Fiz. Tekh. Poluprov. **31**, 432 (1997) [Semicond. **31**, 366 (1997)].
     V. DOBROVOLSKII, I. PALTSEV, and A. ROMANOV, Fiz. Tekh. Poluprov. **31**, 509 (1997) [Semicond. **31**, 431 (1997)].
[13] Z.M. LI, D.J. DAY, S.P MCALISTER, and C.M. HURD, IEEE Electron Devices Lett. **11**, 642 (1990).
[14] D.J. ROBBINS, phys. stat. sol. (b) **97**, 9 (1980); **97**, 387 (1980); **98**, 11 (1980).
[15] C. JACOBONI and P. LUGLI, The Monte Carlo Method for Semiconductor Device Simulation, Springer-Verlag, New York 1989.
[16] P.A. WOLFF, Phys. Rev. **45**, 1415 (1954).
[17] W. SHOCKLEY, Solid State Electronics **2**, 35 (1961).
[18] G.A. BARAFF, Phys. Rev. **128**, 2507 (1962).
[19] B.K. RIDLEY, J. Phys. C **16** 3373 (1987); **16**, 4733 (1987).
     J.S. MARSLAND, Solid State Electronics **30**, 125 (1987).
     R.C. WOOD, IEEE Trans. Electron Devices **34**, 1116 (1987).
     B.K. RIDLEY, Semicond. Sci. Technol. **2**, 116 (1987).
[20] C.R. CROWELL and S.M. SZE, Appl. Phys. Lett. **9**, 242 (1966).
     Y. OKUTO and C.R. CROWELL, Phys. Rev. B **6**, 3076 (1972).
[21] H.F. CHAU and D. PAVLIDIS, J. Appl. Phys. **72**, 531 (1992).
[22] D.M. CAUGHEY and R.E. THOMAS, Proc. IEEE **55**, 2192 (1967).
[23] S.N. MOHAMMAD, Solid State Electronics **35**, 1391 (1992).
[24] J.R. HAUSER, J. Appl. Phys. **37**, 507 (1966).
[25] C.L. ANDERSON and C.R. CROWELL, Phys. Rev. B **5**, 2267 (1972).
[26] J. BUDE and K. HESS, J. Appl. Phys. **72**, 3554 (1992).
[27] A.R. BEATTIE and G. SMITH, phys. stat. sol. **19**, 577 (1967).
     P.T. LANDSBERG, Solid State Commun. **10**, 479 (1972).
     L. HULDT, phys. stat. sol. (a) **24**, 221 (1974).
     P.T. LANDSBERG and D.J. ROBBINS, phys. stat. sol. (b) **97**, 9 (1980).
[28] E. SCHIBLI and A.G. MILNES, Solid State Electronics **11**, 323 (1968).
[29] C.T. SAH and V.G.K. REDDI, IEEE Trans. Electron Devices **11**, 345 (1964).
[30] C.T. SAH and D.K. SCHRODER, Appl. Phys. Lett. **12**, 141 (1968).
[31] C.L. LI, T.M. BARTON, and R.E. MILES, IEEE Trans. Electron Devices **40**, 811 (1993).